Low-energy elastic electron scattering by acetylene

A. Gauf, C. Navarro, G. Balch, L. R. Hargreaves, and M. A. Khakoo
Department of Physics, California State University, Fullerton, California 92834, USA

C. Winstead and V. McKoy
A. A. Noyes Laboratory of Chemical Physics, California Institute of Technology, Pasadena, California 91125, USA
(Received 5 December 2012; published 28 January 2013)

We report measurements and first-principles calculations of the differential cross sections for elastic scattering of low-energy electrons by acetylene, C_2H_2, at collision energies from 1 to 100 eV, with an emphasis on energies near and below that of the π^* shape resonance. The measurements cover angles from 5° to 130°. We compare our results to previous experimental and theoretical values.

DOI: 10.1103/PhysRevA.87.012710 PACS number(s): 34.80.Bm

I. INTRODUCTION

Acetylene, C_2H_2, is a prototypical molecule in several respects. As a readily available gas and one of the smallest and most symmetric polyatomic molecules, it is amenable to both experimental and computational study. It is the smallest member of the important family of unsaturated hydrocarbons and is isoelectronic with N_2, having in common with those molecules both a bonding π_u orbital and an empty π_g antibonding (π^*) orbital that strongly influences photoabsorption, photoionization, and electron-collision spectra. Electron collisions are important in the chemistry of acetylene plasmas [1], and acetylene has been detected in natural environments where free electrons may occur, including the interstellar medium [2] and the atmospheres of Jupiter [3], Saturn and its moon Titan [4], Neptune [5,6], and Uranus [6–8].

Previous experimental and theoretical studies have treated several aspects of electron-acetylene collisions. Karwasz and coworkers [9] have reviewed the body of work up to 2001. Total scattering cross sections were measured at low energies by Brüche [10] and by Sueoka and Mori [11], and, more recently, at intermediate and high energies by Xing and coworkers [12], Ariyasinghe and Powers [13], and Iga and coworkers [14]. Total cross sections above 10 eV have been calculated using a number of simplified models [15–18]. Recently, Vinodkumar and coworkers [19] have computed the total cross section for electron-acetylene scattering from 1 to 5000 eV using a hybrid approach: below 15 eV, they apply the *R*-matrix method, while above 15 eV they use local potentials.

Kochem and coworkers [20] studied the resonant vibrational excitation of acetylene via the $^2\Pi_g$ resonance near 2.5 eV, while Andrić and Hall [21] measured vibrational excitation via both the $^2\Pi_g$ resonance and a $^2\Sigma_g$ resonance at 6 eV, as well as higher-lying Feshbach resonances. Dissociative attachment mediated by the $^2\Pi_g$ resonance has been the subject of several experimental studies [22–26], the most recent and detailed being that of May and coworkers [26], while Chorou and Orel [27,28] have carried out corresponding *ab initio* calculations in which the results agree well with the measurements of May and coworkers. At very low energies, information on the momentum-transfer and vibrational-excitation cross sections has been inferred from drift-tube measurements, most recently by Nakamura [29].

Differential cross sections (DCSs) for elastic scattering of electrons by acetylene have been measured by several groups. In the intermediate-energy range, DCSs were obtained by Fink and coworkers [30] from 100 to 1000 eV and by Iga and coworkers [14] from 50 to 500 eV. At lower energies, the first measurements appear to be those of Hughes and McMillen [31], who obtained relative elastic DCSs from 10 to 100 eV. The study of Kochem and coworkers [20], though primarily focused on vibrational excitation, also produced elastic-scattering data in the low-energy range, including the DCS at 2 eV as a function of scattering angle and the DCS at a fixed angle of 90° as a function of energy between 0 and 3.5 eV. Further results from Kochem and coworkers were quoted in the later paper of Jain [32]. Elastic and vibrationally inelastic DCS measurements from 5 to 100 eV were reported by one of us, Khakoo, and coworkers [33]. However, discrepancies remain between existing measurements at all energies, motivating the present study using improved experimental techniques.

There have been several computational studies of low-energy elastic electron-acetylene scattering. Using local potentials to model the electron-molecule interaction, Thirumalai and coworkers [34] computed DCSs at 10 eV for rotationally elastic and inelastic scattering, as well as the rotationally summed DCS that is directly comparable to typical measurements, in which rotational structure is not resolved. Tossell [35] used a different local-potential approach, namely, the multiple-scattering $X\alpha$ method, to compute the integral cross section in the vicinity of the $^2\Pi_g$ resonance, as well as other properties. Khurana and Jain [36] and Jain [32] likewise applied local model potentials to the problem, reporting results up to 20 eV, while Gianturco and Stoecklin [37] used a similar approach to obtain results up to 50 eV. Using all-electron, *ab initio* methods, Krumbach and coworkers [38] focused on computing cross sections for resonant vibrational excitation, but in the process they obtained results for the energy and width of the $^2\Pi_g$ resonance as a function of the C–C bond distance. We also note studies by Venkatnathan and Mishra [39], using an electron propagator method, and recently by Ghosh and coworkers [40], using coupled-cluster techniques, in which the energy and width of the $^2\Pi_g$ resonance were computed at the equilibrium geometry. Mu-Tao and coworkers [41] used an all-electron formulation, i.e., the iterative Schwinger method,

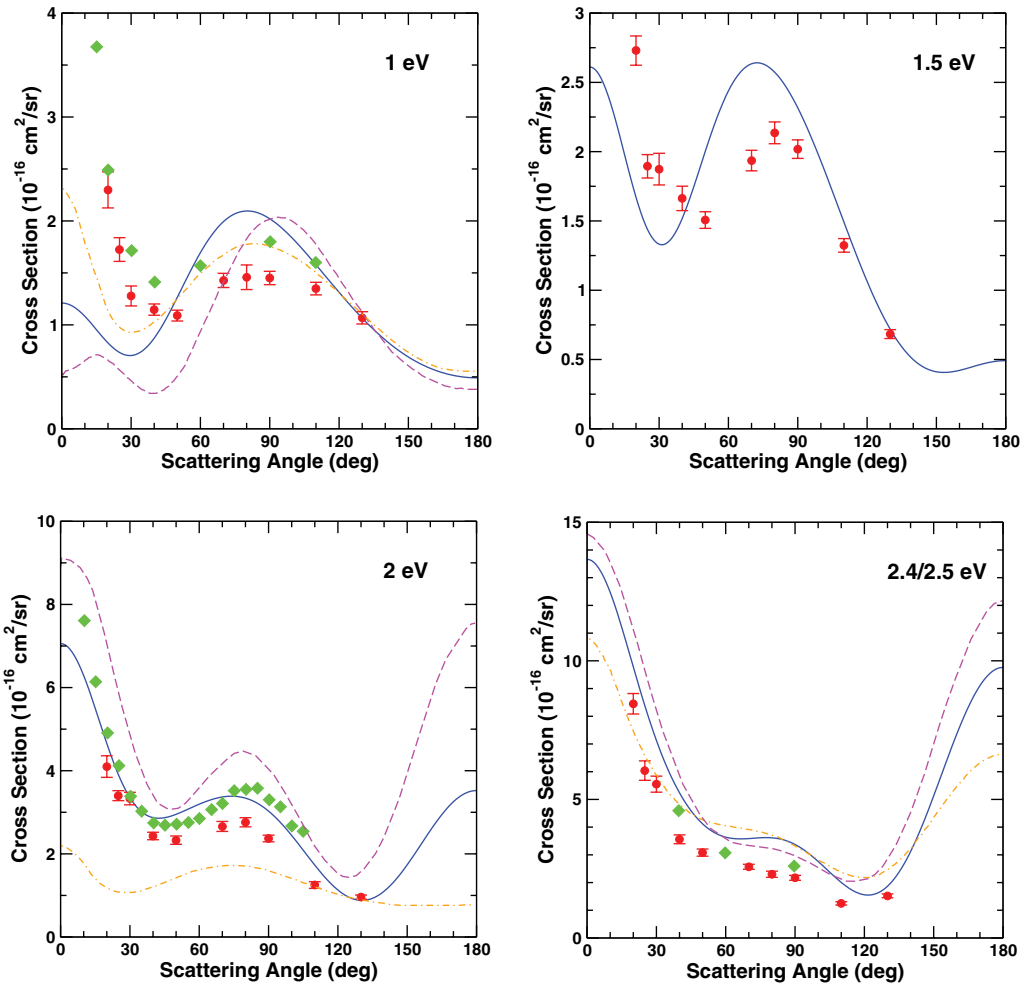

FIG. 1. (Color online) Differential cross section for elastic electron scattering by C_2H_2 at the electron energies indicated in each panel; in the lower right panel, all results are at 2.5 eV except the present calculation. Red circles are the present measurements, and the blue solid line is the present calculation. Also shown are previous calculations by Jain [32] (magenta dashed line) and by Gianturco and Stoecklin [37] (orange dot-dashed line). Green diamonds are the measurements of Kochem and coworkers [20] scaled upward by a factor of 2; except at 2 eV, these results are as quoted in Ref. [32].

to compute cross sections from 10 to 200 eV; more recently, Iga and coworkers [14] extended the calculations of Mu-Tao and coworkers by including local correlation-polarization and absorption potentials, reporting results from 10 to 500 eV. The study of Franz and coworkers [42] primarily treats positron scattering but also includes cross sections for elastic electron-C_2H_2 scattering obtained with two different procedures: one that uses a local correlation-polarization potential based on density functional theory, which they call the DFT model, and the other an all-electron treatment via the R-matrix method. Other computational studies have focused exclusively on positron-acetylene scattering [43–49], with an emphasis on accounting for the vibrational excitation and annihilation observed [50,51] at very low energies.

The principal goal of the present work is to obtain measurements and *ab initio* calculations of the DCSs for elastic electron-acetylene scattering in the energy range below about 5 eV, where the collision process is most sensitive to target polarization and where both the $^2\Pi_g$ resonance and a possible Ramsauer-Townsend minimum [29,32,37] may influence the cross section. Existing experimental data on the elastic cross sections in this region are scant, and the available calculations are not in good quantitative agreement with those data. For completeness, we also report results above 5 eV, thus covering a range of energies from below the $^2\Pi_g$ resonance to well above the ionization potential. We compare with previous measurements and calculations where possible.

II. EXPERIMENT

The experimental apparatus has been described previously, e.g., by Khakoo and coworkers [52], so only a brief description will be given here. The electron gun and the detector employ double hemispherical energy selectors with cylindrical electrostatic lenses, and the apparatus is made of titanium. The system was heated to about 130° C with magnetically free biaxial heaters (ARi Industries, model BXX06B41-4K). The analyzer detector comprised a discrete dynode electron multiplier (Equipe Thermodynamique et Plasmas, model AF151) with the extremely low background rate of <0.01 Hz and the capability of linearly detecting up to 1 MHz of electrons

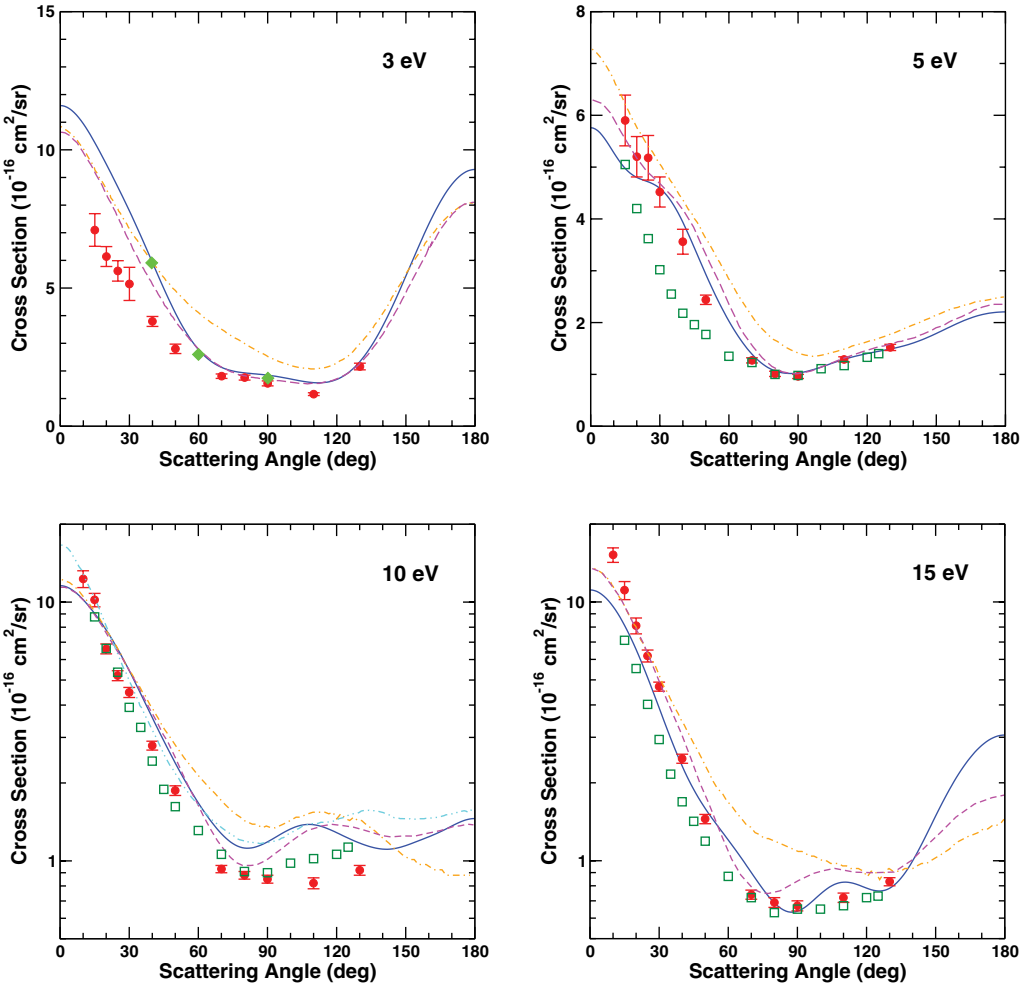

FIG. 2. (Color online) As in Fig. 1, at higher energies. At 5 eV and above, the open green squares show the previous measurements of Khakoo and coworkers [33]. At 10 eV, the cyan double-dot-dashed line is the calculation of Thirumalai and coworkers [34]. The lower panels use a logarithmic vertical scale to make details at larger scattering angles more visible.

without saturating. The analyzer used two virtual apertures downstream from the entrance (0.7 and 1 mm diameter), which enabled a more efficient transmission of low residual energy electrons because these apertures could be operated at a higher energy rather than being fixed at the collision region potential. A skimmer nose piece and a 3 mm aperture at the entrance to this analyzer served to suppress secondary electrons and limited the depth of field of the detector to be ± 3 mm about the collision region. The remnant magnetic field in the collision region is reduced to about 1 mG by using a double μ-metal shield as well as a coil that eliminated the vertical component of the Earth's magnetic field. Typical electron currents were around 20 to 25 nA, with an energy resolution of 50 to 60 meV, full width at half maximum. The electron beam could be focused down to 1.0 eV. The spectrometer current remained stable to within 10% over a period of several weeks, requiring minor tuning of the spectrometer to maintain the long-term stability of the current to within 10% at any time. The energy of the beam was established by determining the dip in the He elastic-scattering cross section due to the $2\,^2S$ He^- resonance at 19.366 eV [53] to an uncertainty of ± 20 meV during a run at a given impact energy E_0. Typically, the contact potential, so determined, was found to be 0.97 ± 0.05 eV over the multiweek course of the experiments. Energy-loss spectra of the elastic peak were collected at fixed energies E_0 and electron scattering angles θ by repetitive, multichannel-scaling techniques. The angular resolution was 2°, full width at half maximum. The effusive target gas beam was formed by flowing gas through a thin aperture source that was 0.3 mm in diameter, described previously [54]. This source was sooted, using an acetylene flame, to reduce secondary electrons and was placed 6 mm below the axis of the electron beam, incorporated into a movable source arrangement [55]. The movable gas source method has been well tested previously in our laboratory and determines background scattering rates expediently and accurately. The vapor pressure behind the source for acetylene was between 0.2 and 0.35 Torr, and that for helium was between 1.0 and 1.6 Torr, while the average pressure in the experimental chamber was about 1×10^{-6} Torr. The gas beam temperature, determined by the apparatus temperature in the collision region, was about 130° C; however, most of the gas-handling copper tubing was at room temperature, about 25° C, with the higher temperature only in the last 4 cm of the gas handling system before the gas exited into the

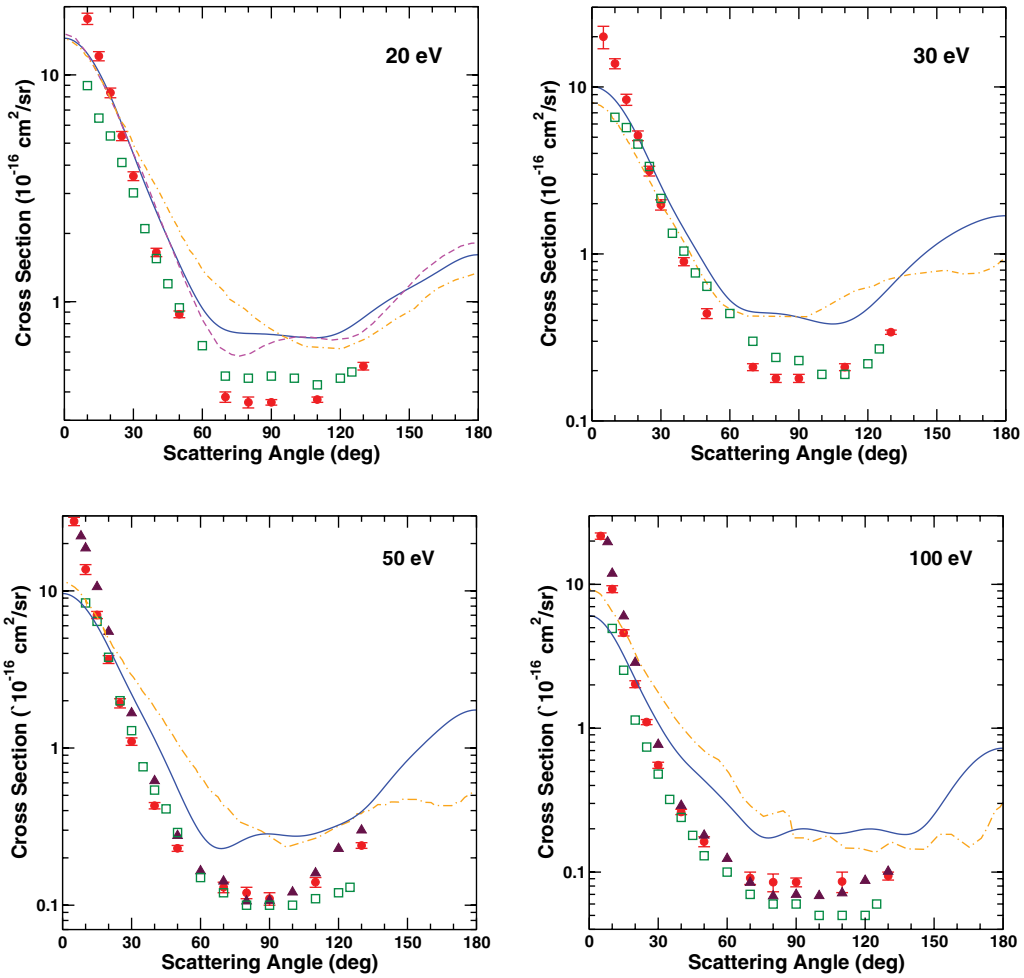

FIG. 3. (Color online) As in Figs. 1 and 2, at higher energies. At 50 and 100 eV, the maroon triangles show the measurements of Iga and coworkers [14]. A logarithmic vertical scale is again used for clarity.

collision region. Based on the flow-rate vs. drive pressure analysis [54], the gas-kinetic molecular diameter of acetylene was determined to be 4.92×10^{-8} cm, close to that of ethylene, i.e., 4.95×10^{-8} cm, at the same temperature [54]. The differential cross sections for elastic scattering from acetylene were normalized via relative flow [54] to the well-established elastic cross sections for He from Nesbet [56].

Our elastic-scattering measurements were taken at E_0 values of 1, 1.5, 2, 2.5, 3, 5, 10, 15, 20, 30, 50, 80, and 100 eV for scattering angles ranging from 5° to 130°. To compute integral elastic and momentum-transfer cross sections, the measured DCSs were extrapolated to 0° and 180° using the present calculation or other available theory as an aid wherever possible and a reasonable visual extrapolation otherwise.

III. COMPUTATIONS

Our calculations used the Schwinger multichannel (SMC) method [57,58] as implemented for parallel computers [59,60]. Because a description of the method may be found in the references cited, we give here only details particular to the present calculations.

Acetylene's ground state is linear, with $D_{\infty h}$ symmetry. All calculations were carried out in the D_{2h} subgroup at the experimental equilibrium geometry [61], for which r(C–C) = 1.203 Å and r(C–H) = 1.063 Å. We used the same one-electron basis set as in earlier work on ethylene [62]. This set includes s Gaussians distributed on a grid of centers to enlarge the "computational box" within which the wave function is represented. Within that basis set, we computed the Hartree-Fock ground state of C_2H_2 using GAMESS [63], and we transformed the Hartree-Fock virtual orbitals into "modified virtual orbitals" (MVOs) [64] using a 4+ cationic Fock operator. Scattering calculations were carried out in the static-exchange plus polarization approximation, with a separate calculation for each irreducible representation of D_{2h}. To describe polarization effects, the trial wave functions included all singlet-coupled single excitations from the five valence orbitals of the Hartree-Fock ground state into the 30 lowest-energy MVOs coupled with all MVOs that would give a 15-electron doublet configuration state function of the appropriate symmetry. In the $^2B_{2g}$ and $^2B_{3g}$ representations, where the $^2\Pi_g$ (π^*) resonance occurs, we also included triplet-coupled single excitations from the two highest occupied orbitals into the two lowest MVOs, i.e., $^3(\pi \rightarrow \pi^*)$, when forming the doublet variational space, because prior experience has shown that, in molecules possessing low-lying triplet excited states, virtual excitations to those states may be critical to

TABLE I. Measured differential cross sections (10^{-16} cm^2/sr) for elastic electron scattering by acetylene. The second column at each energy lists the error estimate. Italicized entries are interpolated or extrapolated values used in computing the integral elastic (σ_I) and momentum-transfer (σ_{MT}) cross sections, which are listed, along with their error estimates, at the foot of the columns in 10^{-16} cm^2 units.

Angle (deg)	1 eV		1.5 eV		2 eV		2.5 eV		3 eV		5 eV		10 eV		15 eV		20 eV		30 eV		50 eV		80 eV		100 eV	
0	*8.0*		*8.0*		*15.0*		*26.0*		*10.5*		*7.6*		*18.56*		*19.24*		*28.0*		*30.0*		*70.0*		*50.0*		*45.0*	
1	*7.5*		*7.5*		*12.0*		*24.0*		*10.0*		*7.2*		*17.92*		*18.37*		*26.0*		*27.0*		*50.0*		*40.0*		*35.0*	
3	*7.0*		*7.0*		*10.0*		*23.0*		*9.5*		*7.10*		*16.64*		*17.49*		*25.0*		*24.0*		*40.0*		*30.0*		*28.0*	
5	*6.0*		*6.0*		*9.0*		*20.0*		*9.0*		*7.10*		*15.36*		*16.18*		*23.0*		20.0	1.6	27.7	2.8	22.8	2.2	21.7	2.0
8	*5.0*		*5.0*		*7.5*		*17.0*		*8.5*		*6.50*		*14.08*		*14.87*		*19.5*		*16.0*		*19.0*		*18.0*		*15.0*	
10	*4.2*		*4.2*		*6.3*		*14.0*		*8.0*		*6.3*		12.3	1.3	13.3	1.4	17.7	1.7	13.8	1.5	13.7	1.5	13.4	1.2	9.27	0.90
15	*3.4*		*3.4*		*5.4*		*10.0*		7.1	0.8	5.9	0.7	10.2	1.0	9.7	1.1	12.1	1.1	8.4	0.9	7.03	0.67	6.68	0.60	4.61	0.44
20	2.3	0.3	2.7	0.2	4.1	0.4	8.5	0.8	6.1	0.6	5.2	0.6	6.6	0.6	7.1	0.8	8.34	0.78	5.11	0.53	3.66	0.36	2.88	0.26	2.03	0.20
25	1.73	0.18	1.89	0.17	3.40	0.30	6.04	0.59	5.62	0.58	5.18	0.60	5.20	0.47	5.41	0.52	5.38	0.50	3.14	0.32	1.93	0.20	1.52	0.14	1.10	0.10
30	1.28	0.14	1.87	0.19	3.33	0.30	5.55	0.53	5.15	0.65	4.52	0.46	4.48	0.41	4.12	0.37	3.58	0.33	1.97	0.21	1.10	0.11	0.75	0.07	0.55	0.05
40	1.15	0.11	1.66	0.16	2.43	0.21	3.56	0.33	3.79	0.35	3.56	0.37	2.79	0.25	2.17	0.20	1.65	0.15	0.90	0.09	0.43	0.04	0.31	0.03	0.26	0.02
50	1.09	0.10	1.51	0.13	2.33	0.21	3.08	0.28	2.80	0.28	2.44	0.21	1.87	0.17	1.26	0.11	0.88	0.08	0.44	0.05	0.23	0.02	0.17	0.02	0.16	0.02
70	1.43	0.13	1.94	0.17	2.66	0.24	2.57	0.23	1.81	0.17	1.27	0.11	0.93	0.08	0.65	0.06	0.38	0.03	0.21	0.02	0.13	0.01	0.084	0.082	0.091	0.012
80	1.46	0.17	2.14	0.19	2.76	0.2	2.30	0.21	1.76	0.17	1.01	0.10	0.88	0.08	0.60	0.05	0.36	0.03	0.18	0.02	0.12	0.01	0.080	0.008	0.085	0.011
90	1.45	0.13	2.02	0.17	2.37	0.21	2.17	0.19	1.55	0.15	0.96	0.09	0.85	0.07	0.58	0.05	0.36	0.03	0.18	0.02	0.11	0.01	0.095	0.011	0.085	0.009
110	1.35	0.12	1.32	0.12	1.25	0.13	1.25	0.12	1.16	0.11	1.29	0.11	0.82	0.08	0.63	0.06	0.37	0.03	0.21	0.02	0.14	0.02	0.11	0.01	0.086	0.012
130	1.07	0.10	0.68	0.06	0.96	0.09	1.52	0.14	2.16	0.21	1.52	0.14	0.92	0.08	0.73	0.06	0.52	0.05	0.34	0.03	0.24	0.02	0.19	0.02	0.094	0.01
140	*1.00*		*0.65*		*0.65*		*1.60*		*2.60*		*1.70*		*0.99*		*0.79*		*0.59*		*0.40*		*0.30*		*0.30*		*0.100*	
150	*0.95*		*0.62*		*0.62*		*1.70*		*2.70*		*1.90*		*1.06*		*0.83*		*0.67*		*0.48*		*0.40*		*0.40*		*0.104*	
160	*0.93*		*0.60*		*0.60*		*1.70*		*2.70*		*2.00*		*1.11*		*0.90*		*0.75*		*0.54*		*0.50*		*0.50*		*0.110*	
170	*0.91*		*0.60*		*0.60*		*1.75*		*2.70*		*2.05*		*1.19*		*0.96*		*0.84*		*0.68*		*0.60*		*0.60*		*0.114*	
180	*0.90*		*0.60*		*0.60*		*1.75*		*2.70*		*2.05*		*1.30*		*1.05*		*0.90*		*0.80*		*0.70*		*0.70*		*0.120*	
σ_I	16.8	2.3	19.3	2.4	25.3	3.2	33.1	4.2	30.1	4.2	24.0	3.4	20.6	2.7	17.2	2.3	15.2	2.0	9.7	1.4	7.9	1.1	6.69	0.86	4.86	0.64
σ_{MT}	15.3	1.8	15.6	1.7	18.4	2.1	23.1	2.6	25.0	3.1	19.6	2.4	12.8	1.5	9.7	1.2	6.86	0.79	4.24	0.53	3.08	0.38	2.67	0.30	1.34	0.16

the description of related elastic-channel resonances. The size of the variational space ranged from 3118 functions in ^2A_u to 3943 in ^2A_g and totaled 28 284 over the eight representations of D_{2h}. The scattering amplitudes for the different representations were summed, squared, and orientationally averaged in the usual way to obtain DCSs appropriate for a gas of randomly oriented molecules.

IV. RESULTS AND DISCUSSION

Our measured and calculated DCSs for elastic scattering of low-energy electrons by acetylene are shown in Figs. 1–3 along with selected results from the literature, and the measured values are also listed in Table I. At energies up to 2.5 eV (Fig. 1), the cross section shows a pronounced d-wave shape, reflecting the influence of the $^2\Pi_g$ resonance. The present measurements are fairly close to those of Kochem and coworkers [20] provided that, as suggested by Jain [32], we scale the latter measurements by a factor of 2. The present calculation is reasonably successful at reproducing the experimental DCS; however, at 1, 1.5, and 2 eV, it is not sufficiently forward peaked, while it is too large at the center of the resonance. Both of these shortcomings likely reflect the calculation's neglect of vibration, which would broaden the resonance and decrease its peak value. Of the previous calculations shown, that of Jain is closest to the present SMC results.

At 3 eV (Fig. 2), the influence of the resonance on the DCS is still apparent. All of the results shown in the figure reflect this shape but differ in detail. In particular, the present calculation agrees well with the present measurements at intermediate angles but is larger, and closer to the scaled results of Kochem and coworkers [20,32], in the forward direction. The angular pattern has changed by 5 eV. The present measurements at 5 eV are considerably different from the earlier experimental data [33] in the forward direction and agree quite well with the present calculation, as well as with that of Jain [32], at almost all angles.

At still higher energies, shown in Figs. 2 and 3, the agreement between experiment and theory deteriorates, as the single-channel approximation used in all of the calculations shown (except that of Thirumalai and coworkers at 10 eV [34]) becomes increasingly inappropriate. However, at 10 and 15 eV, there is still fair agreement at most angles. The disagreement between our present and earlier measurements [33] in the forward-scattering direction is most likely due to the background measurement method used in Ref. [33], where gas was shunted in by a side leak. The movable-source method [55] employed in the present experiment provides a much better background measurement. At the highest energies (Fig. 3), we observe improved agreement with the results of Iga and coworkers [14] over that obtained in our earlier measurements [33], especially at large scattering angles.

Figure 4 shows the differential cross section at a fixed scattering angle of 90° as a function of collision energy. Such "excitation functions" can reveal the presence of resonances that are less clearly seen in angle-integrated data and are also sensitive tests of the agreement between calculations and measurements. In the present case, the $^2\Pi_g$ resonance shows up prominently, though closer to 2.0 than to 2.5 eV, indicating, as already seen in the results of Kochem and coworkers [20,32],

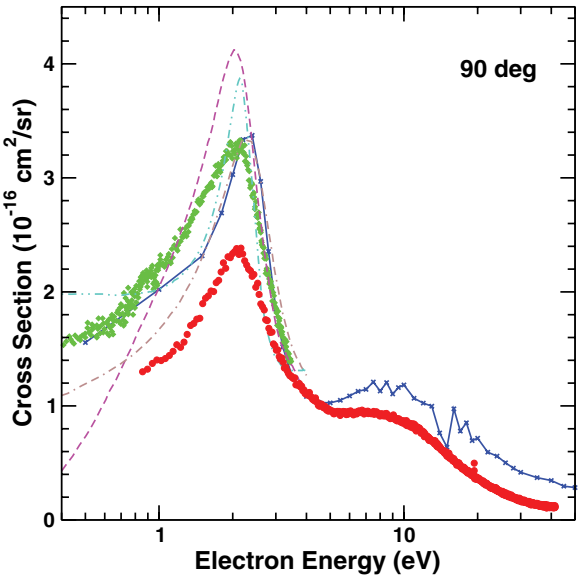

FIG. 4. (Color online) Differential cross section for elastic scattering of electrons by C_2H_2 at a scattering angle of 90°, plotted as a function of energy. Symbols are as in Fig. 1, with the addition of two calculations by Franz and coworkers [42]: the brown dot-dashed line shows their DFT-model results, and the cyan double-dot-dashed line shows their R-matrix results.

that the location of the resonant peak is angle dependent. Fig. 4 also exhibits a broad peak centered at 8.5 eV; as discussed in the next paragraph, this feature appears to be due to a $^2\Sigma_u^+$ resonance. The comparison among the various results shown in Fig. 4 is mixed: The present measurements are in good agreement with those of Kochem and coworkers [20] (scaled by a factor of 2) on the high-energy side of the $^2\Pi_g$ peak, but smaller by about 20% at the peak and by almost a factor of 2 at 1 eV. Likewise, the various calculations agree fairly well with each other, and with the results of Kochem and coworkers, above the $^2\Pi_g$ peak, but diverge from each other at lower energies. The present calculation agrees moderately well with the DFT-model calculation of Franz and coworkers [42] except at the lowest energies, where it agrees better with their R-matrix results and with the scaled data of Kochem and coworkers.

In Figs. 5 and 6, we show the D_{2h} symmetry components of the present calculated integral cross section. The latter figure concentrates on the low-energy region, in which only the ^2A_g ($^2\Sigma_g^+$) and $^2B_{1u}$ ($^2\Sigma_u^+$) components are significant, and it includes, for comparison, results obtained with an expanded "computational box" created by adding diffuse s Gaussians (exponent 0.0092) around the periphery of the original grid (26 points on a 3 × 3 × 3 cubic grid of spacing 9.2 Å, with the point at the origin omitted). The large but nonresonant contribution of $^2\Sigma_u^+$ at these low energies can be understood as due to the large polarizability of acetylene along the C–C axis, with scattering of the p-wave component of B_{1u} producing the backward-peaked DCS that is characteristic of polarization potentials at energies below 1 eV (not shown), even though, as seen in Fig. 1, the shape of the DCS is strongly influenced by the 2.5 eV π^* resonance already by 1 eV. As seen in Fig. 5, the $^2B_{1u}$ contribution to the cross section rises to a broad maximum at about 8.5 eV, and there is also a weak jump in the $^2B_{1u}$

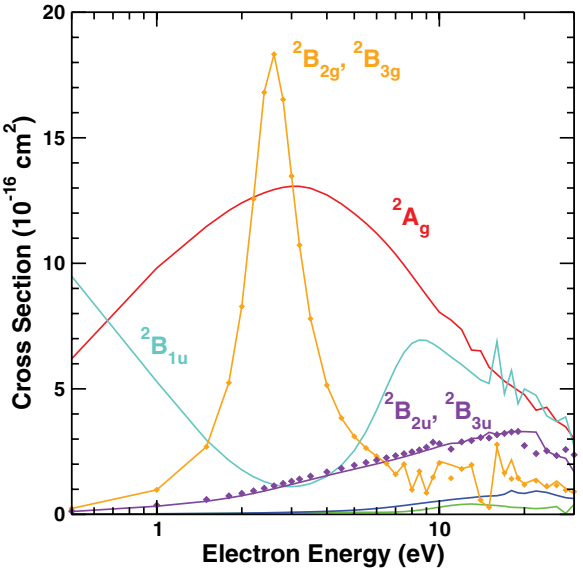

FIG. 5. (Color online) Symmetry components of the present calculated integral elastic cross section for electron scattering by C_2H_2, within the D_{2h} subgroup of $D_{\infty h}$ used in the calculation. The leading $D_{\infty h}$ contributions are $^2\Sigma_g^+$ to ^2A_g, $^2\Sigma_u^+$ to $^2B_{1u}$, $^2\Pi_g$ to $^2B_{2,3g}$, and $^2\Pi_u$ to $^2B_{2,3u}$. The small unlabeled components are $^2B_{1g}$ (upper curve) and ^2A_u (lower curve), for which the leading contributions are $^2\Delta_g$ and $^2\Delta_u$, respectively.

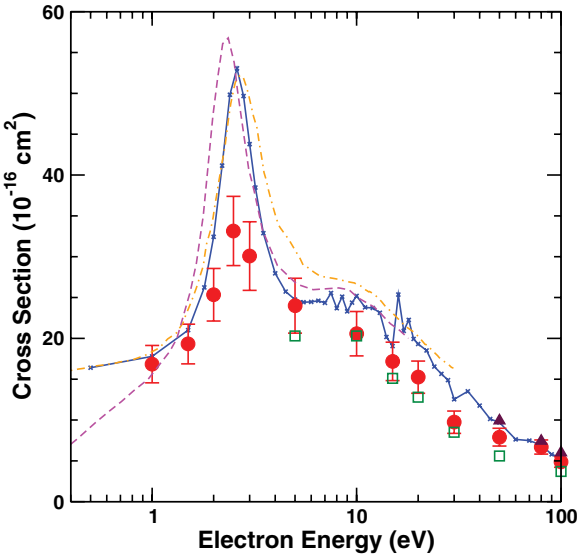

FIG. 7. (Color online) Integral cross section for elastic scattering of electrons by C_2H_2. Red circles are the present measurements, and the blue line is the present calculation. Previous measurements of Khakoo and coworkers [33] are shown by green open squares, and those of Iga and cowokers [14] are shown by maroon triangles. The other calculations shown are those of Jain [32] (dashed magenta line) and of Gianturco and Stoecklin [37] (dot-dashed orange line).

eigenphase sum in the same energy range. These results indicate the presence of a short-lived resonance, most likely a C–C σ^* ($^2\Sigma_u^+$) shape resonance. Indeed, a Hartree-Fock calculation using the MINI basis set as contained in GAMESS [63] puts the lowest virtual valence orbitals at +8.2 eV (π^*) and +14.3 eV (C–C σ^*), and applying to the σ^* energy the same shift of −5.7 eV needed to align the π^* orbital energy with the $^2\Pi_g$ resonance energy yields a prediction of 8.6 eV for the $^2\Sigma_u^+$ (σ^*)

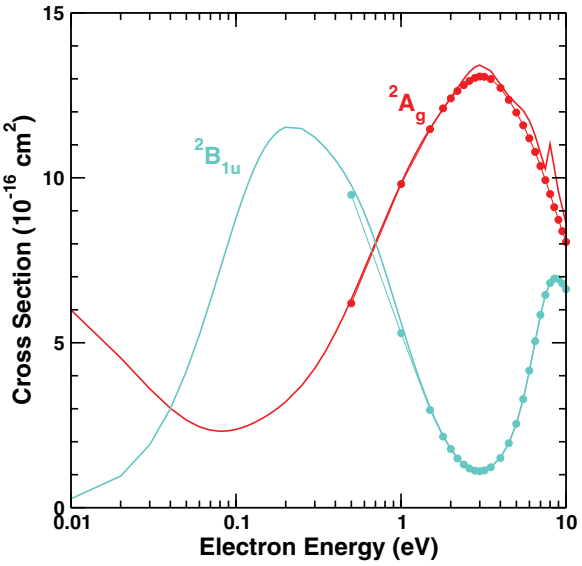

FIG. 6. (Color online) ^2A_g and $^2B_{1u}$ contributions to the integral elastic cross section at low energy. The thin lines with points are the results shown in Fig. 5, and the thicker lines are from an enlarged calculation; see text for discussion.

resonance, in excellent agreement with the position of the feature in the scattering cross section. Note that this resonance does not appear to be the same as that observed in vibrational excitation by Andric and Hall [21] at 6 eV; the isotropic cross sections associated with that feature led Andric and Hall to assign it as a $^2\Sigma_g$ core-excited resonance. It may, however, be the origin of the broad enhancement observed in the transmission spectrum between 7 and 9 eV by Dressler and Allan [25].

Previous studies have indicated the presence of a Ramsauer-Townsend minimum near 0.1 eV [29,37] or 0.2 eV [32]. Our calculation places the minimum in the ^2A_g component at 0.08 eV (Fig. 6); however, because of the rapid increase of the $^2B_{1u}$ contribution at these energies, the minimum in the integral cross section falls lower, at about 0.02 eV. Assuming the ∼0.1 eV location is correct, it is likely that a still more extensive basis set is necessary to converge the $^2B_{1u}$ ($^2\Sigma_u$) contribution at these extremely low energies; however, a fuller analysis would also need to include other components of the cross section, in particular $^2B_{2,3u}$, which contain the p-wave components transverse to the molecular axis and thus may also contribute to long-range scattering from the polarization potential.

Integral cross sections from the present work are shown in Fig. 7, along with previous measured and calculated values. The present measurements agree well with previous values [14,33]. Both the present calculation and previous calculations [32,37] agree reasonably well with experiment on the position of the $^2\Pi_g$ resonance; however, as expected, these fixed-nuclei calculations produce a stronger and narrower peak than is seen in the measured cross section because they neglect both vibrational broadening of the elastic peak and loss of flux to vibrational-excitation channels. Away from the resonance, agreement with experiment is only moderate, with

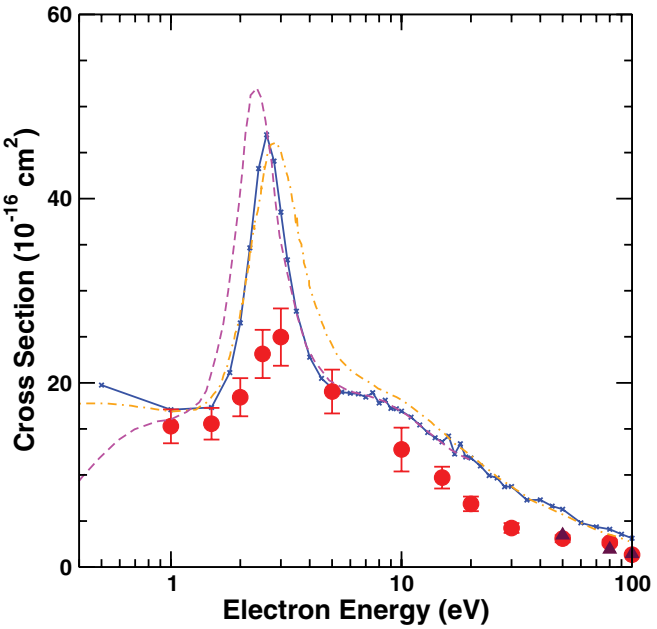

FIG. 8. (Color online) Momentum-transfer cross section for elastic scattering of electrons by C_2H_2. Symbols have the same meanings as in Fig. 7.

the measured values generally somewhat smaller than the calculated values. Above about 6 eV, our calculated integral cross section displays pseudoresonances due to our treatment of all electronic excitation and ionization channels as closed. The overall trends in the momentum-transfer cross section, shown by Fig. 8, are quite similar to those in the integral cross section.

V. CONCLUSIONS

To summarize, the present measurements generally agree well with those of Kochem and coworkers [20,32] in the low-energy region, provided the latter are scaled by a factor of 2, and with the more recent measurements of Iga and coworkers [14] at higher energies, thus putting the elastic electron cross sections of C_2H_2 on a firmer footing over a broad range of incident energies. The present calculations agree modestly well with the measurements and also with earlier calculations, especially that of Jain [32]. The best agreement between calculation and measurement is found immediately below and immediately above the 2.5 eV $^2\Pi_g$ resonance, while known limitations—specifically, neglect of vibrational motion and of electronically inelastic channels—affect both the present and previous theoretical results at the resonance and at higher energies. Together, the present measured and calculated data provide support for the existence of a broad maximum at 8.5 eV due to the $^2\Sigma_u$ shape resonance associated with the C–C σ^* valence orbital.

ACKNOWLEDGMENTS

This work was sponsored by the US National Science Foundation under Grants No. PHY-0968873 and No. PHY-0968874. The work of V.M. and C.W. was supported by the Chemical Sciences, Geosciences and Biosciences Division, Office of Basic Energy Sciences, Office of Science, US Department of Energy under Grant No. DE-FG02-97ER14814 and made use of the Jet Propulsion Laboratory's Supercomputing and Visualization Facility.

[1] J. Benedikt, J. Phys. D **43**, 043001 (2010).
[2] J. H. Lacy, N. J. Evans, J. M. Acthermann, D. E. Bruce, J. F. Arens, and J. S. Carr, Astrophys. J. **342**, L43 (1989).
[3] S. T. Ridgway, Astrophys. J. **187**, L41 (1974).
[4] R. Hanel, B. Conrath, F. M. Flasar, V. Kunde, W. Maguire, J. Pearl, J. Pirraglia, R. Samuelson, L. Herath, M. Allison, D. Cruikshank, D. Gautier, P. Gierasch, L. Horn, R. Koppanay, and C. Ponnamperuma, Science **212**, 192 (1981).
[5] B. Bézard, P. N. Romani, B. J. Conrath, and W. C. Maguire, J. Geophys. Res. **96**, 18961 (1991).
[6] J. I. Lunine, Annu. Rev. Astron. Astrophys. **31**, 217 (1993).
[7] F. Herbert, B. R. Sandel, R. V. Yelle, J. B. Holberg, A. L. Broadfoot, and D. E. Shemansky, J. Geophys. Res. **92**, 15093 (1987).
[8] J. Bishop, S. K. Atreya, F. Herbert, and P. Romani, Icarus **88**, 448 (1990).
[9] G. P. Karwasz, R. S. Brusa, and A. Zecca, Riv. Nuovo Cimento **24**, 1 (2001).
[10] E. Brüche, Ann. Phys. (Leipzig) **394**, 909 (1929).
[11] O. Sueoka and S. Mori, J. Phys. B **22**, 963 (1989).
[12] S. L. Xing, Q. C. Shi, X. J. Chen, K. Z. Xu, B. X. Yang, S. L. Wu, and R. F. Feng, Phys. Rev. A **51**, 414 (1995).
[13] W. M. Ariyasinghe and D. Powers, Phys. Rev. A **66**, 052716 (2002).
[14] I. Iga, M.-T. Lee, P. Rawat, L. M. Brescansin, and L. E. Machado, Eur. Phys. J. D **31**, 45 (2004).
[15] A. Jain and K. L. Baluja, Phys. Rev. A **45**, 202 (1992).
[16] Y. Jiang, J. Sun, and L. Wan, J. Phys. B **30**, 5025 (1997).
[17] D.-H. Shi, Z.-L. Zhu, J.-F. Sun, X.-D. Yang, Y.-F. Liu, and Y. Zhao, Chin. Phys. Lett. **21**, 474 (2004).
[18] D.-H. Shi, J.-F. Sun, H. Ma, Z.-L. Zhu, and X.-D. Yang, Chin. Phys. Lett. **24**, 2819 (2007).
[19] M. Vinodkumar, A. Barot, and B. Antony, J. Chem. Phys. **136**, 184308 (2012).
[20] K.-H. Kochem, W. Sohn, K. Jung, H. Ehrhardt, and E. S. Chang, J. Phys. B **18**, 1253 (1985).
[21] L. Andrić and R. I. Hall, J. Phys. B **21**, 355 (1988).
[22] L. von Trepka and H. Neuert, Z. Naturforsch. A **18**, 1295 (1963).
[23] R. Azria and F. Fiquet-Fayard, J. Phys. (France) **33**, 663 (1972).
[24] R. Abouaf, L. Andrić, R. Azria, and M. Tronc, in *Proceedings of the 12th International Conference on the Physics of Electronic and Atomic Collisions*, edited by S. Datz (North-Holland, Amsterdam, 1981), p. 409.
[25] R. Dressler and M. Allan, J. Chem. Phys. **87**, 4510 (1987).
[26] O. May, J. Fedor, and M. Allan, Phys. Rev. A **80**, 012706 (2009).
[27] S. T. Chourou and A. E. Orel, Phys. Rev. A **77**, 042709 (2008).
[28] S. T. Chourou and A. E. Orel, Phys. Rev. A **80**, 034701 (2009).
[29] Y. Nakamura, J. Phys. D **43**, 365201 (2010).

[30] M. Fink, K. Jost, and D. Herrmann, J. Chem. Phys. **63**, 1985 (1985).
[31] A. L. Hughes and J. H. McMillen, Phys. Rev. **44**, 876 (1933).
[32] A. Jain, J. Phys. B **26**, 4833 (1993).
[33] M. A. Khakoo, T. Jayaweera, S. Wang, and S. Trajmar, J. Phys. B **26**, 4845 (1993).
[34] D. Thirumalai, K. Onda, and D. G. Truhlar, J. Chem. Phys. **74**, 526 (1981).
[35] J. A. Tossell, J. Phys. B **18**, 387 (1985).
[36] I. Khurana and A. Jain, J. Phys. B **25**, L439 (1992).
[37] F. A. Gianturco and T. Stoecklin, J. Phys. B **27**, 5903 (1994).
[38] V. Krumbach, B. M. Nestmann, and S. D. Peyerimhoff, J. Phys. B **22**, 4001 (1989).
[39] A. Venkatnathan and M. K. Mishra, Chem. Phys. Lett. **296**, 223 (1998).
[40] A. Ghosh, N. Vaval, and S. Pal, J. Chem. Phys. **136**, 234110 (2012).
[41] L. Mu-Tao, L. M. Brescansin, M. A. P. Lima, L. E. Machado, and E. P. Leal, J. Phys. B **23**, 4331 (1990).
[42] J. Franz, F. Gianturco, K. Baluja, J. Tennyson, R. Carey, R. Montuoro, R. R. Lucchese, T. Stoecklin, P. Nicholas, and T. Gibson, Nucl. Instrum. Methods B **266**, 425 (2008).
[43] C. R. C. de Carvalho, Márcio T. do N. Varella, M. A. P. Lima, and E. P. da Silva, Phys. Rev. A **68**, 062706 (2003).
[44] T. Nishimura and F. A. Gianturco, Phys. Rev. A **72**, 022706 (2005).
[45] J. Franz and F. A. Gianturco, Eur. Phys. J. D **39**, 407 (2006).
[46] M. T. do N. Varella, E. M. de Oliveira, and M. A. P. Lima, Nucl. Instrum. Methods B **266**, 435 (2008).
[47] S. d'A. Sanchez, M. A. P. Lima, and M. T. do N. Varella, Phys. Rev. A **80**, 052710 (2009).
[48] E. M. de Oliveira, M. A. P. Lima, S. d'A. Sanchez, and Márcio T. do N. Varella, Phys. Rev. A **81**, 012712 (2010).
[49] R. Zhang, P. G. Galiatsatos, and J. Tennyson, J. Phys. B **44**, 195203 (2011).
[50] S. J. Gilbert, L. D. Barnes, J. P. Sullivan, and C. M. Surko, Phys. Rev. Lett. **88**, 043201 (2002).
[51] L. D. Barnes, S. J. Gilbert, and C. M. Surko, Phys. Rev. A **67**, 032706 (2003).
[52] M. A. Khakoo, C. E. Beckmann, S. Trajmar, and G. Csanak, J. Phys. B **27**, 3159 (1994).
[53] J. H. Brunt, G. C. King, and F. H. Read, J. Phys. B **10**, 1289 (1977).
[54] M. A. Khakoo, K. Keane, C. Campbell, N. Guzman, and K. Hazlett, J. Phys. B **40**, 3601 (2007).
[55] M. Hughes, J. K. E. James, J. G. Childers, and M. A. Khakoo, Meas. Sci. Technol. **14**, 841 (1994).
[56] R. K. Nesbet, Phys. Rev. A **20**, 58 (1979).
[57] K. Takatsuka and V. McKoy, Phys. Rev. A **24**, 2473 (1981).
[58] K. Takatsuka and V. McKoy, Phys. Rev. A **30**, 1734 (1984).
[59] C. Winstead and V. McKoy, Adv. At. Mol. Opt. Phys. **36**, 183 (1996).
[60] C. Winstead and V. McKoy, Comput. Phys. Commun. **128**, 386 (2000).
[61] "Computational chemistry comparison and benchmark database," http://cccbdb.nist.gov (unpublished).
[62] C. Winstead, V. McKoy, and M. H. F. Bettega, Phys. Rev. A **72**, 042721 (2005).
[63] M. W. Schmidt, K. K. Baldridge, J. A. Boatz, S. T. Elbert, M. S. Gordon, J. H. Jensen, S. Koseki, N. Matsunaga, K. A. Nguyen, S. Su, T. L. Windus, M. Dupuis, and J. A. Montgomery, J. Comput. Chem. **14**, 1347 (1993).
[64] C. W. Bauschlicher, J. Chem. Phys. **72**, 880 (1980).